Histol Histopathol (2022) 37: 637-654

http://www.hh.um.es

Histology and Histopathology
From Cell Biology to Tissue Engineering

ORIGINAL ARTICLE **Open Access**

Depleting hsa_circ_0000567 suppresses acquired gefitinib resistance and proliferation of lung adenocarcinoma cells through regulating the miR-377-3p / ZFX axis: an *in vitro* and *in vivo* study

Lanjun Wang[1], Mengqi Li[2] and Rong Lian[3]

[1]Central Laboratory, [2]Department of Cardiovascular Division and [3]Department of Otolaryngology, the Fist Affiliated Hospital of Xinxiang Medical College, Weihui, Henan, China

Summary. Background. Circular RNAs (circRNAs) expression profile has been reported in lung adenocarcinoma (LUAD) cells resistant to gefitinib, and hsa_circ_0000567 was abnormally upregulated. However, its precise role in gefitinib resistance remains unclarified.

Methods. Levels of hsa_circ_0000567, microRNA (miR)-377-3p and zinc finger protein X-linked (ZFX) were detected by real-time quantitative PCR. Direct attachment was confirmed by dual-luciferase reporter assay and RNA immunoprecipitation assay. Gefitinib resistance was measured by MTT assay, colony formation assay, flow cytometry, western blotting, and xenograft in mice.

Results. Expression of hsa_circ_0000567 was upregulated in human gefitinib-resistant human LUAD tissues and cells (HCC827/GR and PC9/GR). Clinically, higher hsa_circ_0000567 correlated with advanced tumor burden. Blockage of hsa_circ_0000567 suppressed cell viability, half maximal inhibitory concentration (IC_{50}) value, colony formation ability, and expression of Bcl-2 and proliferating cell nuclear antigen (PCNA) in HCC827/GR and PC9/GR cells under gefitinib treatment or not, accompanied with enhanced apoptosis rate and Bax expression. In vivo, tumor growth of PC9/GR cells untreated and treated with gefitinib was restrained by silencing hsa_circ_0000567. miR-377-3p was directly regulated by hsa_circ_0000567, and then targeted ZFX. Similar to hsa_circ_0000567 knockdown, overexpressing miR-377-3p inhibited chemoresistance in genitinib-resistant LUAD cells in vitro, whereas, depleting miR-377-3p was able to promote gefitinib resistance in spite of hsa_circ_0000567 knockdown. Moreover, restoring ZFX abrogated miR-377-3p-mediated chemosensitivity in genitinib-resistant LUAD cells in vitro.

Conclusion. The hsa_circ_0000567/miR-377-3p/ZFX axis might contribute to acquired gefitinib resistance in LUAD cells both in vitro and in vivo, suggesting hsa_circ_0000567 as a novel therapeutic target in treatment of gefitinib-resistant LUAD.

Key words: hsa_circ_0000567, miR-377-3p, LUAD, Gefitinib resistance, ZFX

Introduction

Non-small-cell lung cancer (NSCLC), the dominant type of lung cancer, is subdivided into lung adenocarcinoma (LUAD), lung squamous cell carcinoma and large-cell lung carcinoma according to histological characteristics (Herbst et al., 2018). Epidermal growth factor receptor (EGFR) gene mutation is the most common genomic driver of NSCLC tumorigenesis, accounting for 51.4% of Asian patients with advanced LUAD (Shi et al., 2014). Tyrosine kinase inhibitors (TKIs) are firmly established as the front-line therapy in 64.8% patients with EGFR-mutated NSCLC (Garg et al., 2020). As one main first-generation TKIs, gefitinib was most frequently selected as the first-line treatment of choice for EGFR mutation-positive NSCLC tumors (Shah and Lester, 2020). However, with time, therapies are often plagued by acquired chemoresistance to the EGFR-TKIs in most patients (60%), including gefitinib (Westover et al., 2018). Accordingly, it is inevitable and imperative to better understand the mechanism of gefitinib resistance in NSCLC.

Very recently, circular RNAs (circRNAs), as newly recognized informative RNAs, have been discovered to participate in tumor development and chemotherapy

Corresponding Author: Lanjun Wang, Central Laboratory, the Fist Affiliated Hospital of Xinxiang Medical College, No.88 Jiankang Road, Weihui 453100, Henan, PR China. e-mail: wljhn0908@126.com
DOI: 10.14670/HH-18-431

resistance in lung cancer (Di et al., 2019). The peculiarity of circRNAs is covalently closed loop structure with neither free 5' caps nor 3' tails, endowing its exceptional structure stability to exoribonuclease digestion. Comprehensive analysis of circRNA expression profiles have been identified in drug-resistant NSCLC (Xu et al., 2018; Chen et al., 2019; Song et al., 2020). hsa_circ_0000567 and hsa_circ_0006867 are key circRNAs in gefitinib-resistant NSCLC cells (Wen et al., 2020); however, their functional role in gefitinib resistance needs to be further highlighted.

Furthermore, the interaction between circRNAs and other non-coding RNAs, particularly microRNAs (miRNAs), has been emerging as popular mechanisms underlying their potential utilities in the development of NSCLC and chemotherapy resistance (Drula et al., 2020). MiRNAs are a class of small single-stranded, endogenous non-coding RNAs with approximately 20~22 nucleotide length, and aberrant miRNA signature has been a mechanism of action of NSCLC progression and metastasis, as well as a drug resistance mechanism of EGFR-mutated NSCLC (Leonetti et al., 2019; Zhu et al., 2021). The circRNAs-miRNAs-messenger RNAs (mRNAs) network has also been constructed (Song et al., 2020; Wen et al., 2020). There are various important miRNAs such as miRNA (miR)-34a (Gupta et al., 2020) and miR-449a (Hu et al., 2021) that can modulate NSCLC proliferation through the induction of apoptosis and cell cycle arrest as well as senescence and autophagy. miR-377-3p is a tumor suppressor in many types of cancers (Wang et al., 2017; Ye et al., 2019; Huang et al., 2020a), including NSCLC (Zhang et al. 2016). Moreover, miR-377-3p has also been associated with gefitinib resistance in LUAD through being regulated by long non-coding RNA SNHG5 and via SNHG5-miR-377-casp1 axis (Wang et al., 2018b). Zinc finger protein X-linked (ZFX) acts as a novel oncogene and a transcriptional activator in various malignancies including NSCLC (Dai et al. 2017; Jiang et al. 2012), and its expression is correlated with malignant phenotypes, including proliferation, tumorigenesis, lymph node status, and patient survival (Jiang et al., 2012; Rhie et al., 2018). Nevertheless, the ZFX role in lung cancer tumorigenesis and development is still poorly understood.

Thus, we intended to shed light on the role of hsa_circ_0000567, a histone methylation-related circRNA (Yu et al., 2020), and miR-377-3p in proliferation and acquired chemoresistance of gefitinib-resistant LUAD cells, and on the possible mechanism associated with hsa_circ_0000567, miR-377-3p and ZFX.

Materials and methods

Clinical tissue specimens

A total of 42 EGFR-mutated LUAD patients (19DEL, L858R and others) were enrolled in this study from The Fist Affiliated Hospital of Xinxiang Medical College. All of the tumor tissues were diagnosed histopathologically by at least two trained pathologists according to the lung tumor classification criteria issued by World Health Organization (2015) (Travis et al., 2015). Tumor tissues and adjacent non-tumor tissues were obtained from surgical specimens. All the participants received no anti-tumor therapy before surgery and standard chemotherapy after surgery. This lung cancer resection was performed following the Declaration of Helsinki, and this study was approved by the Ethics Committee of the Fist Affiliated Hospital of Xinxiang Medical College. The correlations between hsa_circ_0000567 level and clinical characteristics of these 42 patients with LUAD were analyzed and summarized in Table 1.

Cells and gefitinib-resistant cells

Human LUAD cell lines HCC827 (code: 0331) and PC9 (code: 0351) were from BCRJ cell bank in China (Furture Bio, Bejing, China), and cultured in Roswell Part Memorial Institute (RPMI)-1640 medium (Gibco, Carlsbad, CA, USA) supplemented with 10% fetal bovine serum (Gibco). Normal airway epithelial cell line (16HBE; code: SCC150) and 293T cells (code: GDC0187) were provided by Millipore (Bedford, MA, USA) and China Center for Type Culture Collection (Wuhan, China), and cultivated in Dulbecco's modified Eagle's medium (DMEM; Gibco) with high glucose (4500 mg/L) and 10% FBS (Gibco). All cells were

Table 1. The correlations between hsa_circ_0000567 expression and clinical characteristics of 42 patients with LUAD.

Characteristics	n	hsa_circ_0000567 level		P value
		Low	High	
Gender				
Male	25	14	11	0.5303
Female	17	7	10	
Age				
<60	20	7	13	0.1215
≥60	22	14	8	
Smoking history				
Yes	31	17	14	0.4841
No	11	4	7	
EGFR mutation				
L858R	17	7	10	0.8078
T790M	7	3	4	
19DEL	10	6	4	
G719A	5	3	2	
Others	3	2	1	
Tumor size(cm)				0.0001*
<3	26	19	7	
≥3	16	2	14	
TNM stage				0.0005*
I+II	25	18	7	
III+IV	17	3	14	

incubated in humidified air with 5% CO_2 at 37°C.

Gefitinib (code: 184475-35-2; Sigma-Aldrich, Louis, MO, USA) was dissolved in dimethyl sulfoxide (DMSO; Sigma-Aldrich) at a stock concentration of 10 mM and stored at -20°C. HCC827/GR and PC9/GR cells were established by respectively grafting HCC827 and PC-9 cells into gefitinib-containing medium at stepwise increasing concentrations (0.1, 0.5, 1, 5, 10, and 20 μM) for 6 months. The half maximal inhibitory concentration (IC_{50}) of gefitinib in GR cells and the parental cells was calculated using MTT assay, and GR cells showed at least 4-fold higher IC_{50}. The resistant cells were cultured in a gefitinib-free medium for 5 days before all experiments.

Real-time quantitative polymerase chain reaction (RT-qPCR) and circRNA structure identification

Total RNA was extracted in TRIzol reagent (Thermo Fisher Scientific, Waltham, MA, USA) and centrifugation method following the manufacturer's instructions. The RNA quality and quantity were evaluated by NanoDrop 2000 Spectrophotometers (Thermo Fisher Scientific) and denatured agarose gel electrophoresis. RNA samples (500 ng) were reverse-transcribed using High-Capacity cDNA Reverse Transcription kit (Applied Biosystems, Foster City, CA, USA) under standard conditions, and then amplified special RNA expression using different primer pairs and 5× All-In-One RT MasterMix (abm, Richmond, BC, Canada). The internal RNA control was glyceraldehyde-3-phosphate dehydrogenase (GAPDH) and U6, and primer pairs of hsa_circ_0000567, miR-377-3p, ZFX, U6 and GAPDH are presented in Table 2. The relative expressions were calculated using the $2^{-\Delta\Delta Ct}$ method.

For circRNA structure identification, RNA sample (1 μg) from HCC827/GR and PC9/GR cells was incubated with 3 U Ribonuclease R (RNase R; Solarbio, Beijing, China) for 30 min at 37°C. After that, RT-qPCR was utilized to examine hsa_circ_0000567 and GAPDH mRNA expression.

Table 2. The sequence of oligonucleotides and primers.

Gene name	Sequence
hsa_circ_0000567 (146 nt)	Forward: AAACACAGCTCGACAGTACG Reverse: AGCTCACTGGTCAGGTTCAA
si-hsa_circ_0000567#1	Sense: UCUGACUGGAUGACUUUAUAG
si-hsa_circ_0000567#2	Sense: UUCUGACUGGAUGACUUUAUA
si-hsa_circ_0000567#3	Sense: AUUUUUCUGACUGGAUGACUU
sh-hsa_circ_0000567	Sense: TCTGACTGGATGACTTTATAG Antisense: CTATAAAGTCATCCAGTCAGA
ZFX (127 nt)	Forward: TGAGCAAGTGCTGGACTCAG Reverse: ACCCGTCAAGACGTGTTCTG
miR-377-3p (71 nt)	Forward: GCTCACACAAAGGCAACTTTTGTAA Reverse: CTCGCTTCGGCAGCACA
miR-377-3p mimic	Sense: AUCACACAAAGGCAACUUUUGU
miR-377-3p inhibitor	Sense: ACAAAAGUUGCCUUUGUGUGAU
GAPDH (101 nt)	Forward: ATGTTCGTCATGGGTGTGAA Reverse: CAGTGATGGCATGGACTGT
U6 (71 nt)	Forward: CTCGCTTCGGCAGCACA Reverse: AACGCTTCACGAATTTGCGT
si-NC	Sense: CGUACGCGGAAUACUUCGATT
sh-NC	Sense: UUCUCCGAACGUGUCACGU Antisense: ACGUGACACGTTCGGAGAA
mimic NC	Sense: UCUCCGAACGUGUCACGU
inhibitor NC	Sense: CAGUACUUUUGUGUAGUACAA

NC, negative control; nt, nucleotides; GAPDH, Glyceraldehyde 3-phosphate dehydrogenase; si-hsa_circ_0000567, siRNA target hsa_circ_0000567; U6, RNA U6 small nuclear 1; ZFX, Zinc finger protein X-linked.

Cell transfection

The oligonucleotides including siRNAs against hsa_circ_0000567 (si-hsa_circ_0000567#1, #2 and #3), shRNA against hsa_circ_0000567 (sh-hsa_circ_0000567), mimic of miR-377-3p (miR-377-3p mimic), and inhibitor of miR-377-3p (miR-377-3p inhibitor) were self-designed and synthesized by Sangon (Shanghai, China). The sequences of the above oligonucleotides and corresponding negative controls (si-NC, sh-NC, mimic NC, and inhibitor NC) are presented in Table 2. The whole length of coding domain sequence of human ZFX (NM_001178085) was inserted in pcDNA3.11 (+) (pcDNA; Invitrogen, Carlsbad, CA, USA) to construct recombinant pcDNA plasmid, namely pcDNA-ZFX. HCC827/GR and PC9/GR cells were transfected with the above nucleotides with the help of Lipofectamine 3000 reagent (Invitrogen) according to the manufacturers' instructions, and a half dose of nucleotides was used for co-transfection. Cells were harvested after 24 h for further analysis.

MTT assay

After transfection for 24 h, HCC827/GR and PC9/GR cells were grafted in 96-well plates (8000 cells/well) overnight and then treated with gefitinib at concentrations of 0.1, 0.5, 1, 5, 10, and 20 μM for another 24 h. Every concentration group was set up in 5 repeated wells, and 10 μL MTT reagent (Sigma-Aldrich) was applied into the cell culture media. Post-incubation with MTT for 4 h, the supernatants containing MTT were discarded and 150 μL DMSO (Sigma-Aldrich) was added to each well. The optical density was detected at 450 nm by microplate reader. The IC_{50} of gefitinib was calculated.

Flow cytometry (FCM) method

Apoptotic death was measured by FCM method and propidium iodide (PI) single staining combined with fluorescein isothiocyanate (FITC). Transfected HCC827/GR and PC9/GR cells (1×10^5) were treated with 0 and 5 μM gifitinib for 24 h, followed with cell

collection, centrifugation at 2,000 rpm for 5 min, and washing with phosphate buffered saline (PBS). Cells were subjected to Annexin V-FITC apoptosis kit (Beyotime, Beijing, China) and double stained with AnnexinV-FITC and PI for 30 min in the dark according to the instructions. Apoptotic cells were analyzed by S3e flow cytometer (Bio-Rad, Shanghai, China).

Colony formation assay

Transfected HCC827/GR and PC9/GR cells were re-seeded in 6-well plates at a density of 500 cells, and incubated in medium supplemented with 0 and 5 μM gifitinib for another 14 days. The fresh medium was replaced every three days. On the last day, cell colonies formed were washed with ice-cold PBS, fixed with 70% ethanol overnight at 4°C, and then stained with 0.1% crystal violet (Beyotime) for 30 min at room temperature. The stained colonies were visualized and counted under an inverted microscope (Leica, Wetzlar, Germany).

Western blotting

Total protein was isolated from tissues and cells using RIPA regent (Abcam, Cambridge, UK) and centrifugation method at 15,000 g. The supernatant was collected as protein sample, followed with quantification by Bradford method (Thermo Fisher Scientific). After protein separation and transferring, the proteins were labelled with special primary antibodies and secondary antibody. The primary antibodies were targeting Bcl-2 (ab196495; Abcam), Bax (ab182733; Abcam), proliferating cell nuclear antigen (PCNA; ab92729; Abcam), GAPDH (ab181602; Abcam), and ZFX (5405-100; BioVision, Zurich, Switzerland). The secondary antibody HRP-conjugated Mouse anti-rabbit IgG (D110065; Sangon) was used. The signals were detected by ECL-PLUS/Kit (GE Healthcare, Piscataway, NJ, USA) and MYECL™ Imager (Thermo Fisher Scientific).

Xenograft tumor assay

The animal experiment was approved by the Ethics Committee of the Fist Affiliated Hospital of Xinxiang Medical College and performed in accordance with the guidelines of the National Animal Care and Ethics Institution. A total of 20 male athymic BALB/c nude mice (4-5-week-old) were purchased from Laboratory Animal Center of Nanjing University (Nanjing, China) and maintained in specific pathogen-free conditions. PC9/GR cells were stably transfected with sh-hsa_circ_0000567 or sh-NC, and the cell suspension (1×10^6 cells) was subcutaneously injected into the right anterior axilla. Gefitinib or equal volume of normal saline was injected into xenograft tumors at 7th day, and gefitinib was administered by oral gavage every 3.5 days at a dose of 20 mg/kg (n=5). The long diameter (L, mm) and short diameter (S, mm) were measured by caliper every 7 days, and the weight of tumors was measured using electronic balance on the last day. The volume was calculated using $0.5\times L\times S^2$ equation. This animal study was performed accordance with the recommendations in the Care and Use of Laboratory Animals (2006) from Ministry of Science and Technology of China. The tumor tissues were collected and stored at -80°C.

Dual-luciferase reporter assay

The full-length of hsa_circ_0000567 and 3'untranslated region of ZFX (ZFX 3'UTR) were respectively amplified by PCR method and inserted into the downstream of pGL3 luciferase vectors (Promega, Madison, WI, USA) between HindIII and XhoI restriction sites, thus the wild-type plasmids were constructed and named as hsa_circ_0000567 wt and ZFX 3'UTR wt. The predicted binding sites in hsa_circ_0000567 and ZFX 3'UTR were mutated using QuikChange XL SiteDirected Mutagenesis Kit (Agilent Technologies, Palo Alto, CA, USA). Similarly, the mutant plasmids were established and named as hsa_circ_0000567 mut and ZFX 3'UTR mut. Afterwards, 293T cells were co-transfected with the above plasmid and miR-377-3p mimic or mimic NC for 24 h; eventually, the cells were lysed and the luciferase activity was determined by the dual-luciferase reporter assay system (Promega).

RNA immunoprecipitation (RIP) assay

HCC827/GR and PC9/GR cells were subjected to EZ-magna RIP kit (Millipore) according to the working manual. Briefly, cell lysate in RIP buffer was incubated with magnetic beads conjugated with antibody against argonaute 2 (anti-Ago2; ab32381, Abcam) or anti-IgG (ab2410, Abcam) for 12 h at 4°C. The beads were eluted and digested with proteinase K. Then, extracted immunoprecipitated contents were lysed in TRIzol and analyzed by RT-qPCR.

Statistical analysis

Statistical analyses were performed on GraphPad Prism 6 (GraphPad Software, La Jolla, CA, USA) depending on the statistical data (mean ± standard deviation) at least three biological repetitions. Unpaired Student's t-test or one-way analysis of variance followed with Tukey's post-hoc analysis was employed to analyze the statistical difference, and P values of less than 0.05 were deemed as statistically significant. Pearson's correlation analysis was applied to analyze statistical correlation between miR-377-3p and either hsa_circ_0000567 or ZFX mRNA expression levels.

Results

hsa_circ_0000567 was upregulated in gefitinib-resistant LUAD patients and cells

To validate the expression of hsa_circ_0000567 in gefitinib-resistant LUAD tumors, a group of 42 LUAD patients were recruited and classified into gefitinib-resistant and gefitinib-sensitive groups. RT-qPCR data showed higher level of hsa_circ_0000567 in human LUAD tissues than adjacent normal tissues (Fig. 1A), and elevated hsa_circ_0000567 was observed in gefitinib-resistant tumors (Fig. 1B). In addition, hsa_circ_0000567 expression was upregulated from human LUAD cells (HCC827 and PC9) to LUAD cells acquired with gefitinib resistance (HCC827/GR and PC9/GR) (Fig. 1C). hsa_circ_0000567 is a circRNA originating from the back-splicing of SETD3 exon 2-exon 6 (Fig. 1D). Moreover, hsa_circ_0000567 was resistant to RNase R digestion in HCC827/GR and PC9/GR cells, as indicated by no loss of hsa_circ_0000567 level after RNase R treatment which was not consistent with GAPDH mRNA (Fig. 1E).

Depleting hsa_circ_0000567 suppressed acquired gefitinib resistance and proliferation of gefitinib-resistant LUAD cells in vitro via induction of apoptosis

Since hsa_circ_0000567 had been confirmed to be abnormally upregulated in gefitinib-resistant LUAD tissues and cells, siRNAs were utilized to silence its expression. The optimal knockdown efficiency of siRNAs targeting hsa_circ_0000567 was si-hsa_circ_0000567#1 in both HCC827/GR and PC9/GR cells (Fig. 2A), thus si-hsa_circ_0000567#1 was chosen for further loss-of-function experiments. MTT assay depicted a cell viability inhibition in gefitinib-treated HCC827/GR and PC9/GR cells with hsa_circ_0000567 silencing, accompanied with decreased IC_{50} of gefitinib in HCC827/GR cells (from 13.23 μM to 3.113 μM) and

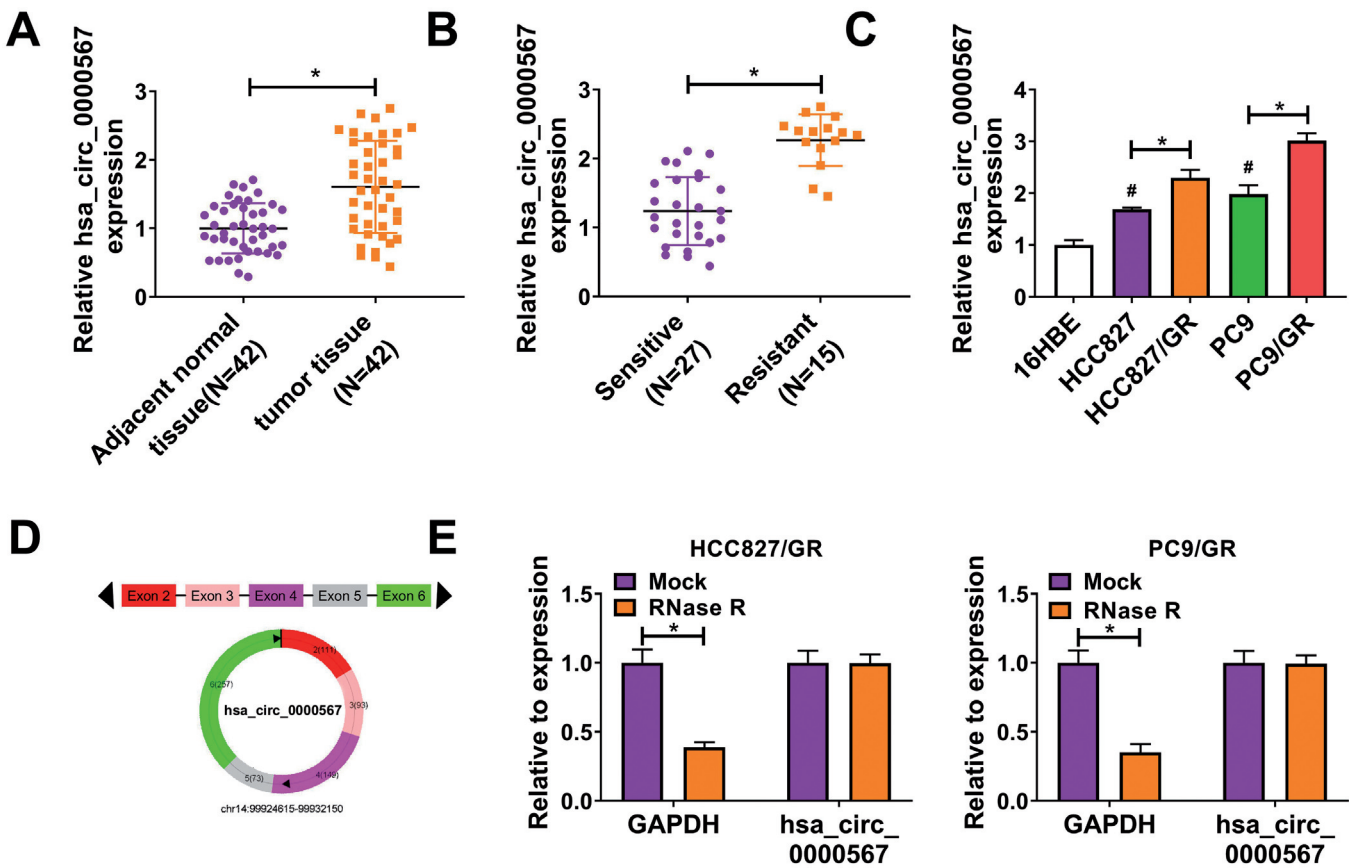

Fig. 1. Expression model of hsa_circ_0000567 in gefitinib-resistant LUAD patients and cells. **A, B.** RT-qPCR detected expression of hsa_circ_0000567 in 42 paired LUAD tumor tissues and adjacent normal tissues **(A)**, and 15 gefitinib-resistant tumors and 27 gefitinib-sensitive tumors **(B)**. *P<0.05 compared with normal or sensitive tissues. **C.** RT-qPCR detected hsa_circ_0000567 expression in human LUAD cell lines (HCC827 and PC9), LUAD cell lines with acquired gefitinib resistance (HCC827/GR and PC9/GR), and normal airway epithelial cell line (16HBE). *P<0.05 compared with sensitive cells, and #P<0.05 compared with normal cells. **D.** Schematic diagram shows the covalently closed structure of hsa_circ_0000567 originating from the back-splicing of exons. **E.** RT-qPCR measured expression of hsa_circ_0000567 and GAPDH mRNA in mock-treated and RNase R-treated HCC827/GR and PC9/GR cells. *P<0.05 compared with mock cells.

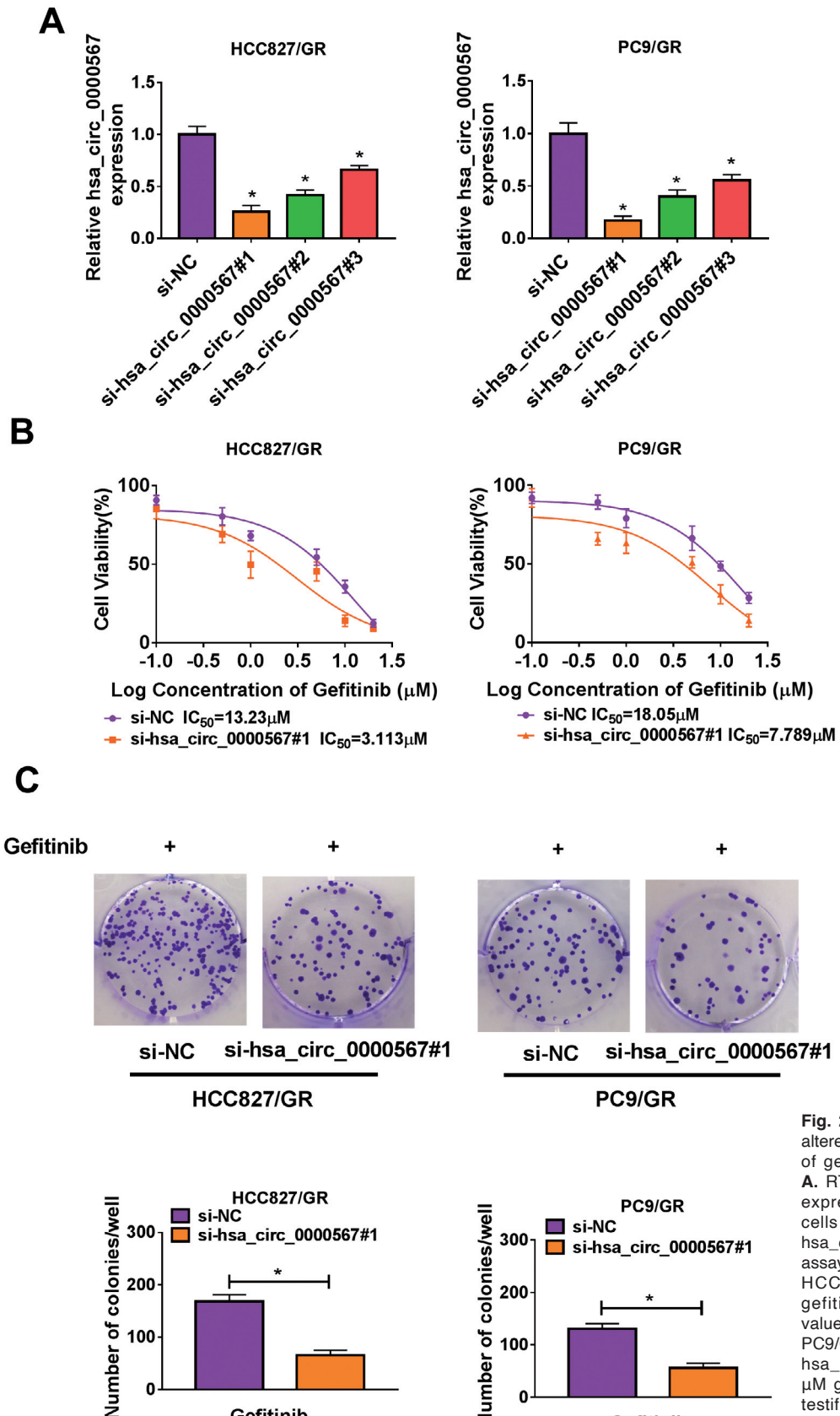

Fig. 2. Dysregulation of hsa_circ_0000567 altered gefitinib resistance and proliferation of gefitinib-resistant LUAD cells *in vitro*. **A.** RT-qPCR measured hsa_circ_0000567 expression in HCC827/GR and PC9/GR cells transfected with siRNAs (si-NC, si-hsa_circ_0000567#1, #2 and #3). **B.** MTT assay evaluated cell viability of transfected HCC827/GR and PC9/GR cells with gefitinib (0-20 μM) treatment, and IC_{50} value was calculated. **C.** HCC827/GR and PC9/GR cells transfected with si-NC or si-hsa_circ_0000567#1 were treated with 5 μM gefitinib, and colony formation assay testified the number of colonies. *P<0.05 compared with si-NC group.

PC9/GR cells (from 18.05 μM to 7.789 μM) (Fig. 2B). Blocking hsa_circ_0000567 suppressed colony formation ability of HCC827/GR and PC9/GR cells with 5 μM gefitinib treatment (Fig. 2C). The FCM method manifested an increase of apoptosis rate in hsa_circ_0000567-silenced HCC827/GR and PC9/GR cells under gefitinib (5 μM) stress (Fig. 3A), which paralleled with elevated Bax expression and diminished Bcl-2 and PCNA expression (Fig. 3B). These results together demonstrated that acquired gefitinib resistance and proliferation of gefitinib-resistant LUAD cells in vitro were able to be restrained by depleting

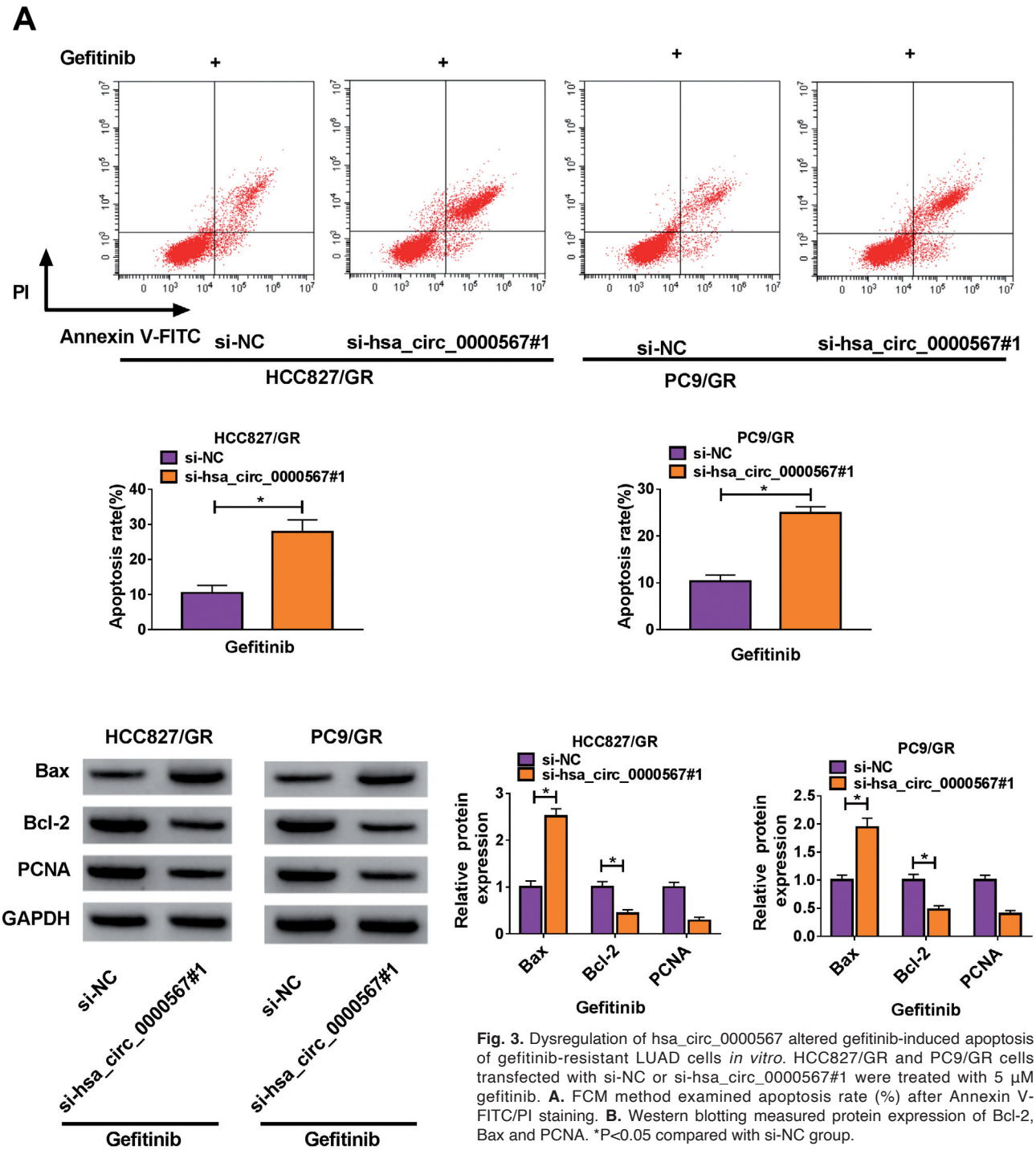

Fig. 3. Dysregulation of hsa_circ_0000567 altered gefitinib-induced apoptosis of gefitinib-resistant LUAD cells *in vitro*. HCC827/GR and PC9/GR cells transfected with si-NC or si-hsa_circ_0000567#1 were treated with 5 μM gefitinib. **A.** FCM method examined apoptosis rate (%) after Annexin V-FITC/PI staining. **B.** Western blotting measured protein expression of Bcl-2, Bax and PCNA. *P<0.05 compared with si-NC group.

hsa_circ_0000567 and via apoptosis promotion.

Silencing hsa_circ_0000567 suppressed acquired gefitinib resistance and tumor growth of gefitinib-resistant LUAD cells in vivo

Furthermore, the effect of hsa_circ_0000567 on gefitinib resistance in vivo was explored in xenograft mice. hsa_circ_0000567-silenced PC9/GR cells were used to induce tumor growth in nude mice, which was then treated with gefitinib or normal saline. Tumor volume and weight were restrained by sh-hsa_circ_0000567 introduction either with gefitinib treatment or not (Fig. 4A,B). Molecularly, sh-hsa_circ_0000567 transfection caused a low expression of hsa_circ_0000567 in xenograft tumors in both gefitinib treatment group and normal saline control group, and meanwhile Bcl-2 and PCNA were depressed and Bax was promoted (Fig. 4C,D). These data proposed a suppression of hsa_circ_0000567 knockdown on tumor growth and acquired gefitinib resistance of gefitinib-resistant LUAD cells in vivo.

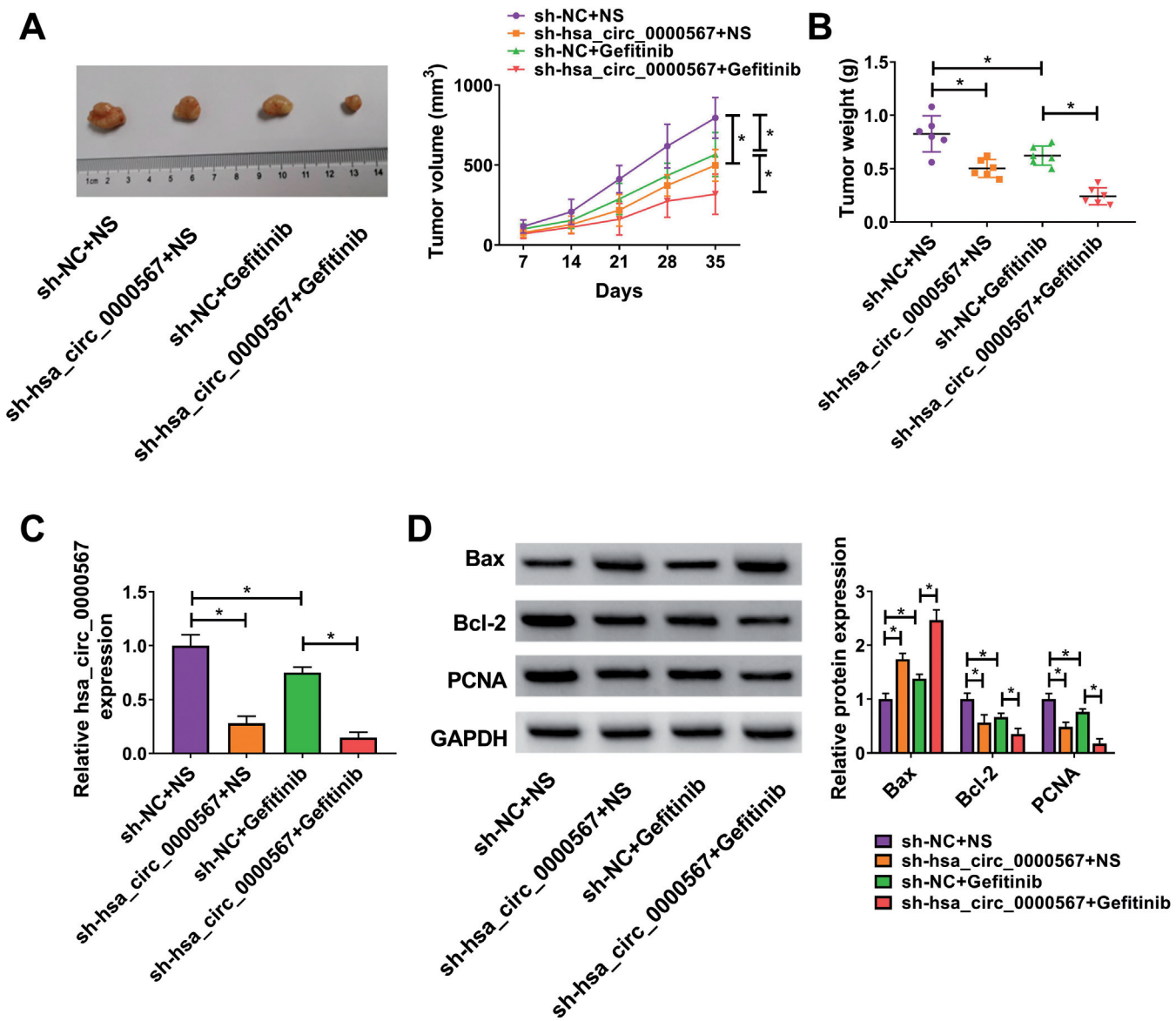

Fig. 4. Dysregulation of hsa_circ_0000567 altered tumor growth and gefitinib resistance of gefitinib-resistant LUAD cells *in vivo*. PC9/GR cells stably transfected with sh-NC or sh-hsa_circ_0000567 were inoculated into nude mice to induce tumor growth, and treated with gefitinib (Gefitinib) or normal saline (NS) (n=5). **A.** Representative tumor images were presented and tumor volume was monitored every 7 days. **B.** Tumor weight was measured after cell inoculation for 35 days. **C.** RT-qPCR detected hsa_circ_0000567 expression, and western blotting detected Bcl-2 **(D)**, Bax and PCNA protein expression in xenograft tumor tissues. *P<0.05 compared with sh-NC+NS or sh-NC+Gefitinib group.

hsa_circ_0000567 directly targeted miR-377-3p in gefitinib-resistant LUAD cells

According to our data, hsa_circ_0000567 deficiency functioned in a tumor-suppressive role in gefitinib-resistant LUAD cells, so the underlying mechanism was further sought out. Target miRNAs of hsa_circ_0000567 were searched on databases, and starbase2.0 (http://starbase.sysu.edu.cn/circRNA&miRNA/=hsa_circ_0000567) and circinteractome (https://circinteractome.nia.nih.gov/mirna target sites search/=hsa_circ_0000567) predicted a panel of 6 miRNAs that showed binding sites in hsa_circ_0000567 (Fig. 5A). Among them, miR-377-3p, miR-488-3p, miR-545-3p, and miR-660 were downregulated in LUAD tumors, accompanied with miR-149-5p and miR-421 upregulation (Fig. 5B). Blocking hsa_circ_0000567 using si-hsa_circ_0000567#1 transfection led to the most upregulation of miR-377-3p in both HCC827/GR and PC9/GR cells (Fig. 5C). Thereby, miR-377-3p was selected as the optimal candidate target for further validation. RT-qPCR analysis showed that miR-377-3p was downregulated from human LUAD tumor tissues and cells to gefitinib-resistant LUAD tissues and cells (Fig. 5D-F). Moreover, miR-377-3p expression was inversely correlated to hsa_circ_0000567 in LUAD patients, as determined by Pearson's correlation coefficient analysis (r=-0.8001 and P<0.001; Fig. 5G). The potential miR-377-3p-binding

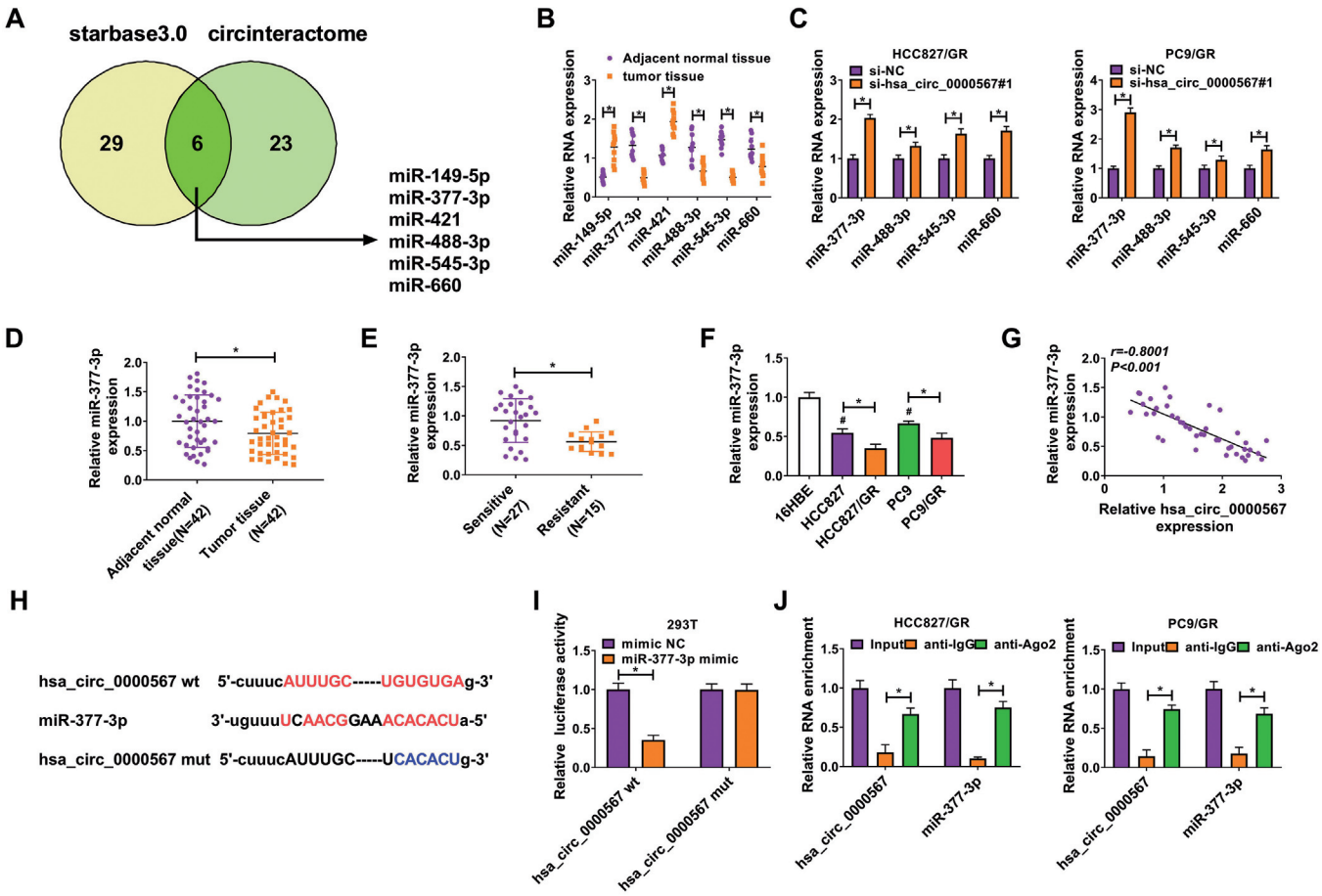

Fig. 5. The direct attachment between hsa_circ_0000567 and miR-377-3p in gefitinib-resistant LUAD cells. **A.** Databases starbase2.0 and circinteractome predicted miRNA binding sites in hsa_circ_0000567. **B.** RT-qPCR detected expression of miRNAs in tumor tissues and adjacent normal tissues from 10 LUAD patients, and (C) HCC827/GR and PC9/GR cells transfected with si-NC or si-hsa_circ_0000567#1 **(C)**. *P<0.05 compared with normal tissue or si-NC-transfected cells. **D, E.** RT-qPCR detected expression of miR-377-3p in (D) 42 paired LUAD tumor tissues and adjacent normal tissues, and 15 gefitinib-resistant LAD tumors and 27 gefitinib-sensitive LUAD tumors **(E)**. *P<0.05 compared with normal or sensitive tissues. **F.** RT-qPCR detected miR-377-3p expression in HCC827 and PC9 (gefitinib-sensitive), HCC827/GR and PC9/GR (gefitinib-resistant), and 16HBE (normal) cells. *P<0.05 compared with sensitive cells, and #P<0.05 compared with normal cells. **G.** Pearson's correlation coefficient analysis analyzed statistical correlation between hsa_circ_0000567 and miR-377-3p expression in LUAD tumors. **H.** Schematic diagram showed the potential binding sites between hsa_circ_0000567 wt and miR-377-3p, as well as the mutated sites in hsa_circ_0000567 mut. **I.** Dual-luciferase reporter assay determined luciferase activity in 293T cells co-transfected with hsa_circ_0000567 report vectors (wt and mut) and miR-377-3p mimic or mimic NC. *P<0.05 compared with mimic NC group. **J.** RIP assay identified the enrichment of hsa_circ_0000567 and miR-377-3p in immunoprecipitated RNAs mediated by anti-Ago2 or anti-IgG in HCC827/GR and PC9/GR cells. *P<0.05 compared with anti-IgG group.

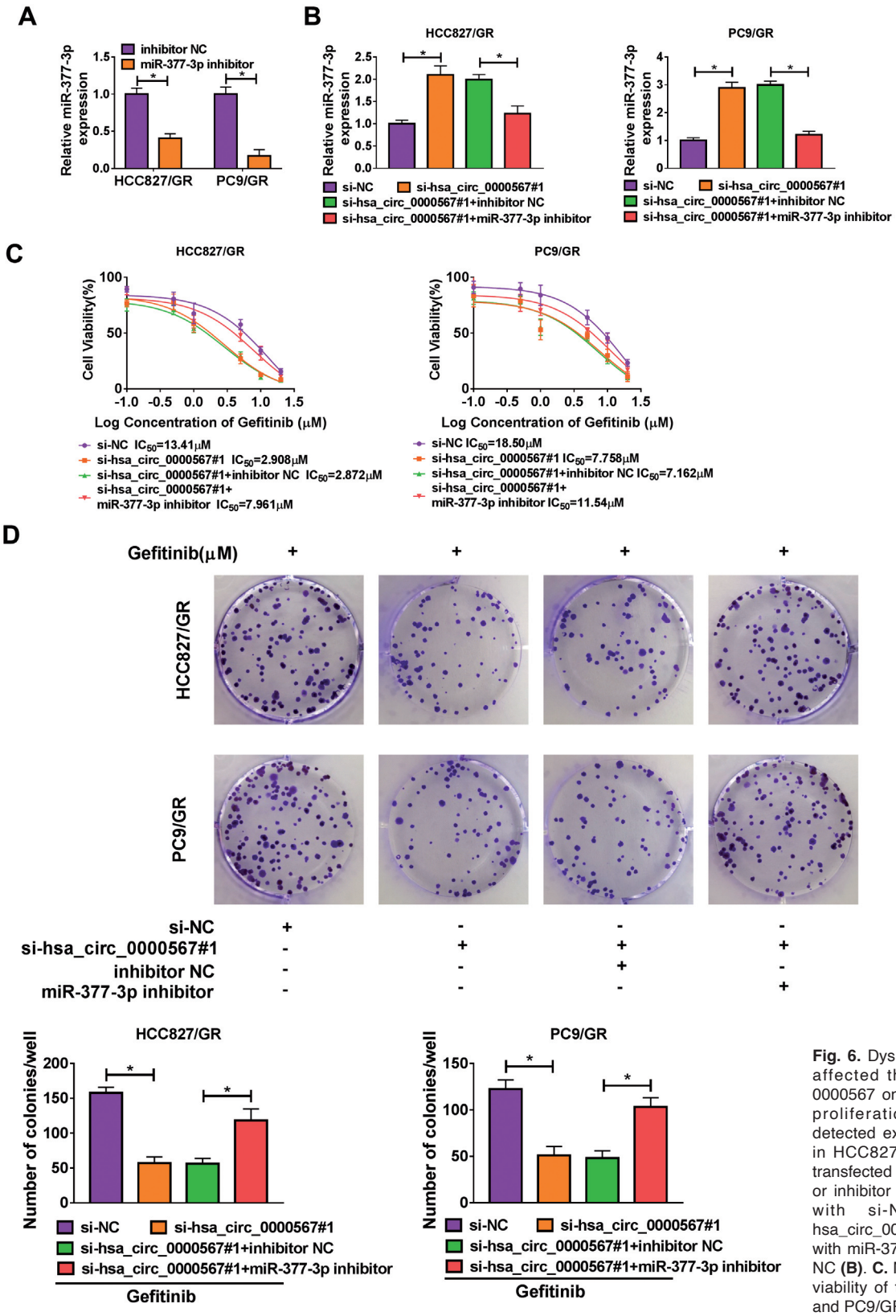

Fig. 6. Dysregulation of miR-377-3p affected the effect of hsa_circ_0000567 on gefitinib resistance and proliferation. **A, B.** RT-qPCR detected expression of miR-377-3p in HCC827/GR and PC9/GR cells transfected with miR-377-3p inhibitor or inhibitor NC **(A)**, and transfected with si-NC alone and si-hsa_circ_0000567#1 alone or along with miR-377-3p inhibitor or inhibitor NC **(B)**. **C.** MTT assay evaluated cell viability of transfected HCC827/GR and PC9/GR cells with gefitinib (0-20 μM) treatment, and IC_{50} value was calculated. **D.** Transfected HCC827/GR and PC9/GR cells were treated with 5 μM gefitinib, and colony formation assay testified the number of colonies **(D)**. *P<0.05 compared with si-NC group or si-hsa_circ_0000567#1+inhibitor NC group.

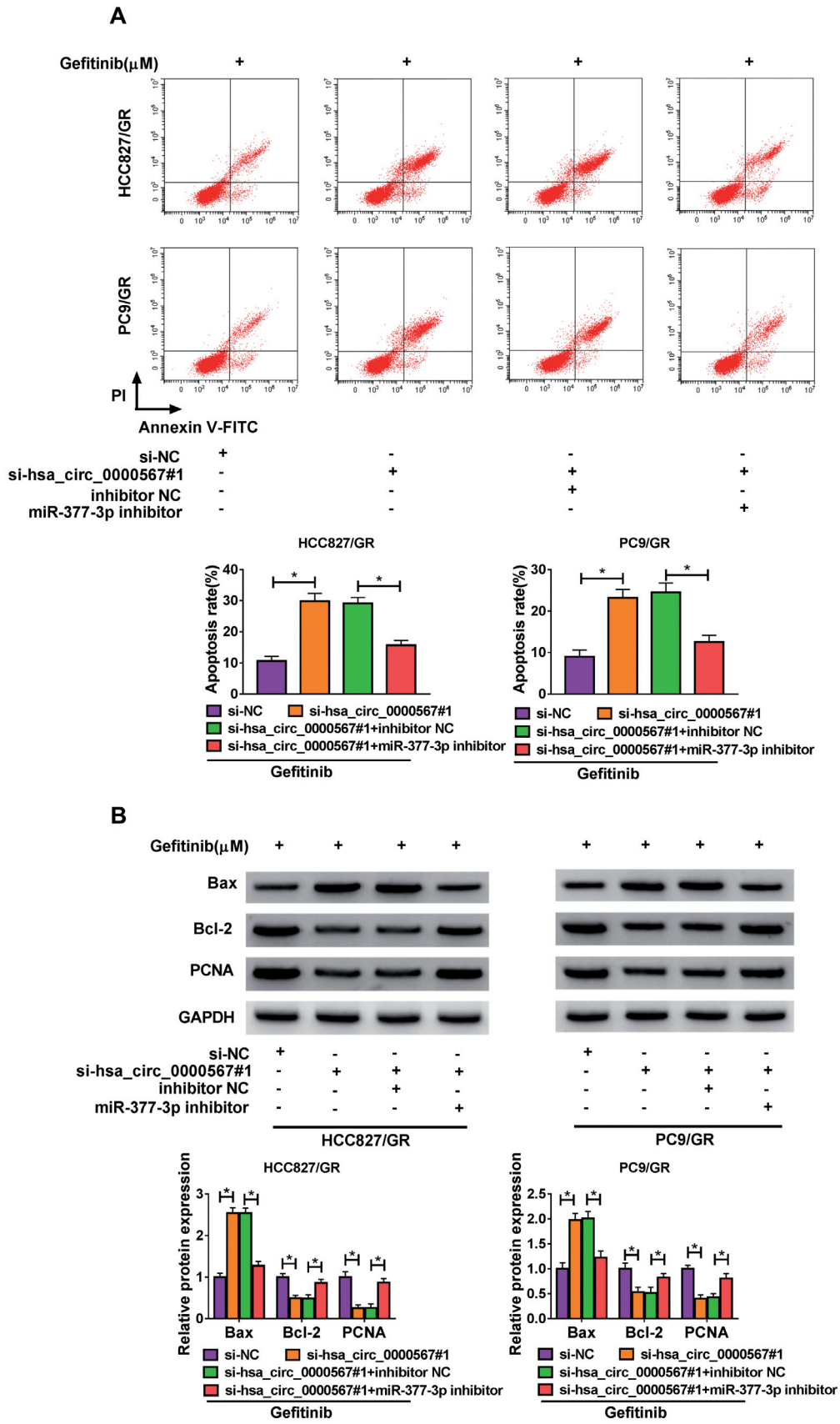

Fig. 7. Dysregulation of miR-377-3p affected the effect of hsa_circ_0000567 on gefitinib-induced apoptosis. HCC827/GR and PC9/GR cells were transfected with si-NC alone and si-hsa_circ_0000567#1 alone or along with miR-377-3p inhibitor or inhibitor NC. **A.** FCM method and Annexin V-FITC/PI staining examined apoptosis rate (%). **B.** Western blotting measured protein expression of Bcl-2, Bax and PCNA. *P<0.05 compared with si-NC group or si-hsa_circ_0000567#1+inhibitor NC group.

sites in hsa_circ_0000567 were mutated (Fig. 5H), and luciferase activity of hsa_circ_0000567 wt report vector was greatly declined while hsa_circ_0000567 mut report vector was not attenuated by the presence of miR-377-3p mimic in 293T cells (Fig. 5I). Besides, hsa_circ_0000567 and miR-377-3p were co-enriched by Ago2-mediated RIP in both HCC827/GR and PC9/GR cells (Fig. 5J). These results demonstrated that miR-377-3p could probably be sponged by hsa_circ_0000567 in gefitinib-resistant LUAD cells.

Inhibiting miR-377-3p counteracted the suppressive effect of hsa_circ_0000567 depletion in gefitinib-resistant LUAD cells in vitro

miR-377-3p inhibitor transfection caused miR-377-3p inhibition (Fig. 6A), and subsequently exhibited a series of effects in HCC827/GR and PC9/GR cells with hsa_circ_0000567 depletion. First of all, si-hsa_circ_0000567#1 administration upregulated miR-377-3p expression, and this upregulation was attenuated with miR-377-3p inhibitor addition (Fig. 6B). The diminished cell viability and IC_{50} of gefitinib in hsa_circ_0000567-silenced HCC827/GR and PC9/GR cells were improved by additional silencing of miR-377-3p (Fig. 6C). Depleting hsa_circ_0000567 inhibited colony formation number of HCC827/GR and PC9/GR cells, which was partially abolished with miR-377-3p inhibitor transfection (Fig. 6D). Apoptosis rate and Bax expression were enhanced, whereas Bcl-2 and PCNA expression declined with si-hsa_circ_0000567#1 sole transfection, and si-hsa_circ_0000567#1 co-transfection

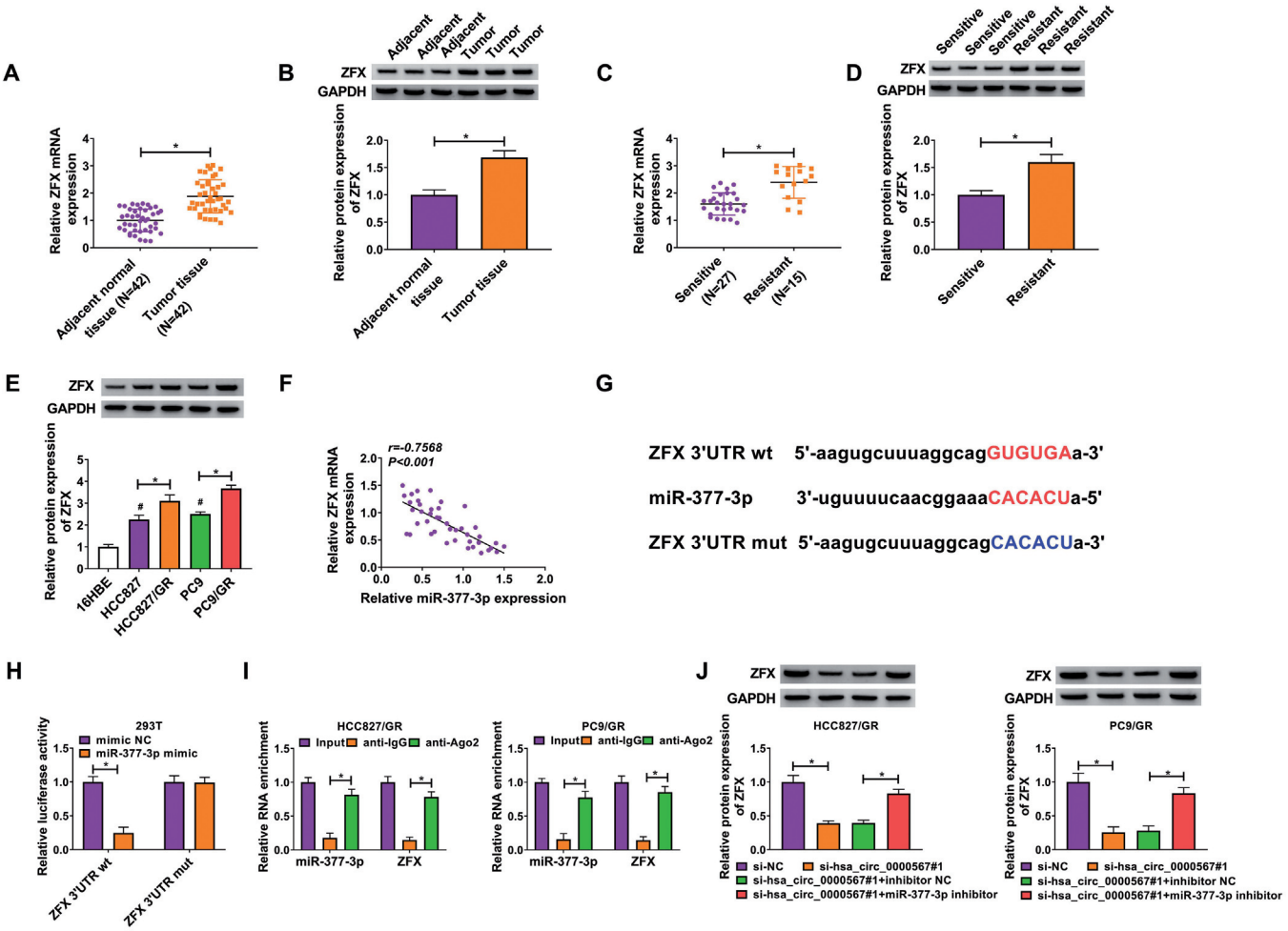

Fig. 8. Expression of ZFX in LUAD and its interaction with miR-377-3p. **A-E.** RT-qPCR and western blotting detected mRNA and protein expression of ZFX in human LUAD tumor and paired normal tissues **(A, B)**, gefitinib-resistant and -sensitive tumors **(C, D)**. *P<0.05 compared with normal or sensitive tissues, and in cell lines HCC827, PC9, HCC827/GR, PC9/GR **(E)**, and 16HBE. *P<0.05 compared with parental cells, and #P<0.05 compared with 16HBE cells. **F.** Pearson's correlation coefficient analysis analyzed statistical correlation between miR-377-3p and ZFX mRNA expression in LUAD patients. **G.** Schematic diagram shows the potential binding sites between miR-377-3p and ZFX 3'UTR wt, as well as the mutated sites in ZFX 3'UTR mut. **H.** Dual-luciferase reporter assay determined luciferase activity in 293T cells co-transfected with ZFX 3'UTR report vectors (wt and mut) and miR-377-3p mimic or mimic NC. *P<0.05 compared with mimic NC group. **I.** RIP assay identified the enrichment of miR-377-3p and ZFX in immunoprecipitated RNAs mediated by anti-Ago2 or anti-IgG in HCC827/GR and PC9/GR cells. *P<0.05 compared with anti-IgG group. **J.** Western blotting measured ZFX protein expression in HCC827/GR and PC9/GR cells transfected with si-NC alone and si-hsa_circ_0000567#1 alone or along with miR-377-3p inhibitor or inhibitor NC. *P<0.05 compared with si-NC group or si-hsa_circ_0000567#1+inhibitor NC group.

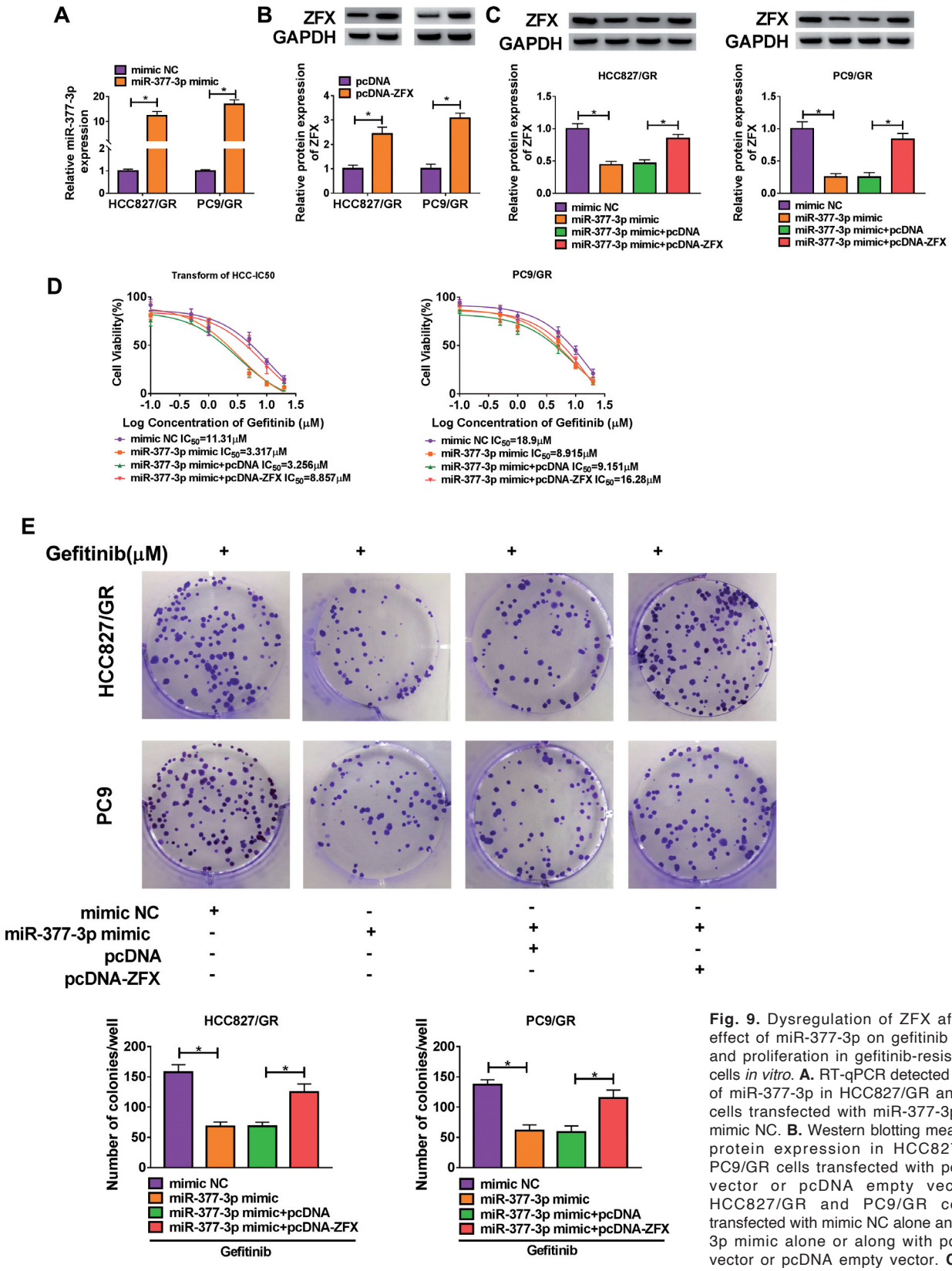

Fig. 9. Dysregulation of ZFX affected the effect of miR-377-3p on gefitinib resistance and proliferation in gefitinib-resistant LUAD cells *in vitro*. **A.** RT-qPCR detected expression of miR-377-3p in HCC827/GR and PC9/GR cells transfected with miR-377-3p mimic or mimic NC. **B.** Western blotting measured ZFX protein expression in HCC827/GR and PC9/GR cells transfected with pcDNA-ZFX vector or pcDNA empty vector. **C-E.** HCC827/GR and PC9/GR cells were transfected with mimic NC alone and miR-377-3p mimic alone or along with pcDNA-ZFX vector or pcDNA empty vector. **C.** Western blotting measured ZFX protein expression. **D.** MTT assay evaluated cell viability with gefitinib (0-20 μM) treatment, and IC_{50} value was calculated. **E.** Colony formation assay testified the number of colonies. *P<0.05 compared with mimic NC group or miR-377-3p mimic+pcDNA group.

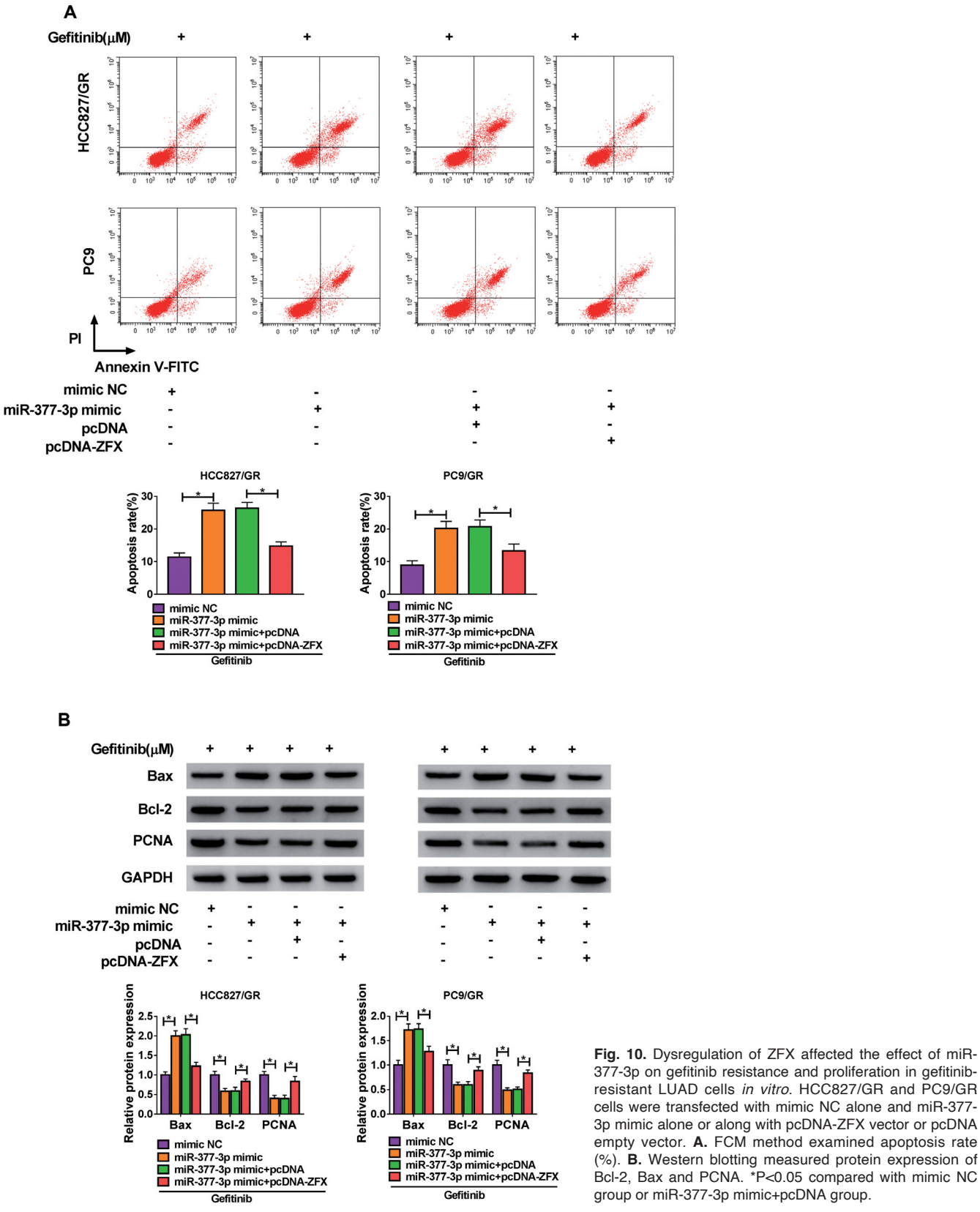

Fig. 10. Dysregulation of ZFX affected the effect of miR-377-3p on gefitinib resistance and proliferation in gefitinib-resistant LUAD cells *in vitro*. HCC827/GR and PC9/GR cells were transfected with mimic NC alone and miR-377-3p mimic alone or along with pcDNA-ZFX vector or pcDNA empty vector. **A.** FCM method examined apoptosis rate (%). **B.** Western blotting measured protein expression of Bcl-2, Bax and PCNA. *P<0.05 compared with mimic NC group or miR-377-3p mimic+pcDNA group.

with miR-377-3p inhibitor was able to partially reverse these effects (Fig. 7A,B). These outcomes depicted a diminishing effect of miR-377-3p silencing on hsa_circ_0000567 depletion effects in gefitinib-resistant LUAD cells in vitro.

ZFX was upregulated in gefitinib-resistant LUAD patients and cells, and was targeted by miR-377-3p

ZFX was a star gene correlated with proliferation, tumorigenesis, and patient survival in multiple types of human cancers (Rhie et al., 2018). Here, RT-qPCR and western blotting assays revealed an upregulation of ZFX in human LUAD tumors (Fig. 8A,B); ZFX mRNA and protein levels were even higher in gefitinib-resistant human LUAD tumors (Fig. 8C,D). Consistently, its expression was upreguated in HCC827/GR and PC9/GR cells compared to the parental cells (Fig. 8E). There was an inverse correlation between miR-377-3p and ZFX mRNA expression in these LUAD patients (Fig. 8F). Starbase2.0 database (http://starbase.sysu.edu.cn/mRNA&miRNA/=hsa-miR-377-3p&clipNum/=ZFX) predicted the potential binding sites between miR-377-3p and ZFX 3'UTR (Fig. 8G). Dual-luciferase reporter assay showed significant reduction of luciferase activity in 293T cells co-transfected with ZFX 3'UTR wt and miR-377-3p mimic (Fig. 8H). Co-enrichment of miR-377-3p and ZFX mRNA by Ago2 was noticed in both HCC827/GR and PC9/GR cells (Fig. 8I). miR-377-3p inhibitor not only abrogated the promoting effect of hsa_circ_0000567 deficiency on miR-377-3p expression (Fig. 6B), but also cancelled its inhibitory effect on ZFX protein expression (Fig. 8J). These results demonstrated that ZFX as a target of miR-377-3p was regulated by both hsa_circ_0000567 and miR-377-3p in gefitinib-resistant LUAD cells.

Restoring ZFX abolished the diminishing effect of miR-377-3p overexpression in gefitinib-resistant LUAD cells in vitro

miR-377-3p mimic introduction induced high expression of miR-377-3p along with low expression of ZFX (Fig. 9A,C), and ectopic expression of AFX via pcDNA-ZFX vector transfection rescued ZFX expression in spite of miR-377-3p mimic in HCC827/GR and PC9/GR cells (Fig. 9B,C). IC_{50} of gefitinib was decreased by overexpressing miR-377-3p from 11.31 μM to 3.317 μM in HCC827/GR cells and from 18.9 μM to 8.915 μM in PC9/GR cells (Fig. 9D). Upregulating miR-377-3p suppressed colony formation number of HCC827/GR and PC9/GR cells treated with 5 μM gefitinib (Fig. 9E). Apoptosis rate was increased in miR-377-3p-overexpressed HCC827/GR and PC9/GR cells under gefitinib (5 μM) stress (Fig. 10A), paralleled with elevated Bax expression and depressed Bcl-2 and PCNA expression (Fig. 10B). These results also disclosed a suppressive role of miR-377-3p upregulation in acquired gefitinib resistance in LUAD cells in vitro through inhibiting ZFX.

Discussion

CircRNA expression profiles in gefitinib-resistant NSCLC cells had been explored compared to their parental sensitive cells, and hsa_circ_0000567 was consistently upregulated in both HCC827/GR (2.3-fold) and PC9/GR (3.5-fold) cells (Wen et al., 2020). hsa_circ_0000567 was a promising diagnostic and prognostic biomarker in hepatocellular carcinoma and colorectal cancer (Wang et al., 2018a, 2019a). These outcomes might indicate a potential dysfunction of hsa_circ_0000567 in lung cancers. Here, we further identified this circRNA expression in gefitinib-resistant patients and cells, accompanied with investigation of its role in cell proliferation and gefitinib resistance both in vitro and in vivo. Moreover, miR-1226-5p, miR-762, miR-593-5p, miR-149-5p, and miR-939-3p were predicted as the top target miRNAs for hsa_circ_0000567 through directly regulating diverse mRNAs involved in gefitinib resistance (Wen et al., 2020). Thus, we further identified its mechanism though functioning as an miRNA sponge.

Unsurprisingly, expression of hsa_circ_0000567 was upregulated from human LUAD tumor tissues and cells to gefitinib-resistant human tissues and cells according to RT-qPCR analysis, which was consistent with the upregulation data in plasmas of gefitinib-resistant NSCLC patients and gefitinib-resistant cells, as well as their culture supernatants (Huang et al., 2020b). These data could conclude hsa_circ_0000567 as a potential biomarker for gefitinib therapy resistance in NSCLC. Incidentally, its expression level was lower in tumor tissues from hepatocellular carcinoma patients and colorectal cancer cases (Wang et al., 2018a, 2019a). Therefore, it can be concluded that hsa_circ_0000567 is differently expressed in different types of human cancer in a content-dependent manner. Besides, its cellular expression was observed to be stable under RNase R digestion and Actinomycin D treatment in this study, which was in agreement with previous studies (Wang et al. 2018a, 2019a; Huang et al. 2020b). In function, silencing hsa_circ_0000567 via siRNA transfection was able to increase gefitinib-induced apoptosis and decrease cell viability and IC_{50} value in HCC827/GR and PC9/GR cells and tumor growth of PC9/GR cells in vivo, and these outcomes had already been better elucidated via overexpression assays in gefitinib-sensitive cells (PC9 and HCC827), or knockdown assays in gefitinib-resistant cells (HCC827/GR and PC9/GR). Additionally, we further discovered that colony formation ability of gefitinib-resistant LUAD cells was depressed by interfering hsa_circ_0000567, and that and tumor growth of PC9/GR cells was delayed whether gefitinib treatment was processed or not. Collectively, depleting hsa_circ_0000567 can be a potential approach to interfere with gefitinib therapy resistance for LUAD, and our data further enhanced the knowledge of the anti-

growth role of hsa_circ_0000567 depletion in gefitinib-resistant LUAD cells. Therefore, it could be concluded that hsa_circ_0000567 was a promising therapeutic target for acquired resistance to gefitinib in NSCLC, especially LUAD. However, its relationship to clinical characteristics of LUAD patients remains to be further analyzed, such as tumor size, lymph metastasis, tumor-node-metastasis (TNM) stage, and overall survival.

Mechanically, circRNAs-miRNAs-mRNAs interaction network underlying hsa_circ_0000567 was predicted and validated, as previously demonstrated (Wang et al., 2019a; Huang et al., 2020b; Wen et al., 2020). As a result, hsa_circ_0000567 was confirmed as an miR-377-3p sponge to further regulate ZFX, a novel downstream target of miR-377-3p. miR-377-3p was an abnormally downregulated miRNA in NSCLC patients and cells (Zhang et al., 2016, 2017; Sun et al., 2016; Wang et al., 2019b; Li et al., 2020). Here, we observed that miR-377-3p was lowly expressed in human LUAD tissues and cells, and even lower in gefitinib-resistant human LUAD tissues and cells. Furthermore, its expression was correlated with hsa_circ_0000567 in LUAD patients recruited in this present study. miR-377-3p was implicated in regulation of gefitinib resistance in PC9 and PC9/GR cells (Wang et al., 2018b); whereas, its detailed role in gefitinib resistance was undisclosed in that study. Here, we discovered that upregulating miR-377-3p was able to reverse gefitinib resistance in HCC827/GR and PC9/GR cells by regulating cell viability, IC_{50}, colony formation, and apoptosis. Also, blocking miR-377-3p alleviated the suppression of hsa_circ_0000567 knockdown on grfitinib resistance and proliferation of LUAD cells in vitro. Cell migration and invasion were not covered in this study, and needed to be illuminated in another investigation in the future. More importantly, a high risk of three novel competing endogenous RNA (ceRNA) interactions including SNHG1-hsa-miR-377-3p-RALGPS2 was positively associated with worse prognosis (Tan et al., 2020).

ZFX was overexpressed and correlated with malignant phenotype of NSCLC, including lymph node status in NSCLC patients, as stated by Jiang et al. (2012) and Zha et al. (2013). Here, we observed that ZFX was highly expressed in human LUAD tissues and cells, and even higher in gefitinib-resistant human LUAD tissues and cells. ZFX restoration was able to modulate apoptosis related proteins Bax, Bcl2 and PCNA in gefitinib-resistant LUAD tissues and cells, and many other proteins were also regulated by ZFX in NSCLC cells, including Ki-67, Survivin, caspase-3, and Cyt c (Li et al., 2013; Zha et al., 2013). In terms of chemoresistance, ZFX has been little studied in human cancers, expect for cisplatin resistance in hepatocellular carcinoma (Lai et al., 2014), imatinib resistance in leukemia (Wu et al., 2016), and castration resistance in prostate cancer (Cai et al., 2018). In lung cancers, this study might be a pioneer in ZFX regulation in chemoresistance.

MiR-377-3p was able to target multiple functional genes involved in chemoresistance and tumor cell proliferation in NSCLC, such as CASP1 (Wang et al., 2018b), ADAM metallopeptidase domain 28 (Zhong et al., 2021) and glutamate oxaloacetate transaminase 1 (Zhu et al., 2020), and Starbase2.0 database showed thousands of miR-377-3p potential targets which remain to be further verified. Furthermore, ZFX can influence transcriptional regulation of many genes by acting as a transcriptional activator (Rhie et al., 2018). These outcomes suggested a complex regulatory network of circ_0000567/miR-377-3p interplay; however, this study provided ZFX as a new member in this ceRNA network.

All in all, this study demonstrated that hsa_circ_0000567 knockdown functioned in an anti-tumor role and gefitinib-sensitive role in LUAD cells by inhibiting proliferation and promoting apoptosis both in vitro and in vivo via the miR-377-3p/ZFX axis. We propose hsa_circ_0000567 as a potential therapeutic target in gefitinib-resistant LUAD, and hsa_circ_0000567/miR-377-3p/ZFX ceRNA pathway as a promising mechanism.

Authors' contribution. LW designed and supervised the study, conducted the experiments and drafted the manuscript. ML involved in methodology development. RL collected and analyzed the data, edited the manuscript. All authors read and approved the final manuscript.

Data Availability Statement. The analyzed data sets generated during the study are available from the corresponding author on reasonable request.

Competing interest. The authors report no conflicts of interest in this work.

Funding. There is no funding to report.

References

Cai L., Tsai Y.H., Wang P., Wang J., Li D., Fan H., Zhao Y., Bareja R., Lu R., Wilson E.M., Sboner A., Whang Y.E., Zheng D., Parker J.S., Earp H.S. and Wang G.G. (2018). ZFX mediates non-canonical oncogenic functions of the androgen receptor splice variant 7 in castrate-resistant prostate cancer. Mol. Cell 72, 341-354 e346.

Chen T., Luo J., Gu Y., Huang J., Luo Q. and Yang Y. (2019). Comprehensive analysis of circular RNA profiling in AZD9291-resistant non-small cell lung cancer cell lines. Thorac. Cancer 10, 930-941.

Dai C., Dong Q., Lu Q., Liu F.T. and Zhu Z.M. (2017). Prognostic value of Zinc-finger protein X-linked in patients with solid tumors. Minerva Chir. 72, 81-88.

Di X., Jin X., Li R., Zhao M. and Wang K. (2019). CircRNAs and lung cancer: Biomarkers and master regulators. Life Sci. 220, 177-185.

Drula R., Braicu C., Harangus A., Nabavi S.M., Trif M., Slaby O., Ionescu C., Irimie A. and Berindan-Neagoe I. (2020). Critical function of circular RNAs in lung cancer. Wiley Interdiscip. Rev. RNA 11, e1592.

Garg A., Batra U., Choudhary P., Jain D., Khurana S., Malik P.S., Muthu V., Prasad K.T., Singh N., Suri T. and Mohan A. (2020). Clinical predictors of response to EGFR-tyrosine kinase inhibitors in EGFR-mutated non-small cell lung cancer: A real-world multicentric cohort analysis from India. Curr. Probl. Cancer 44, 100570.

Gupta S., Silveira D.A., Barbe-Tuana F.M. and Mombach J.C.M. (2020). Integrative data modeling from lung and lymphatic cancer predicts functional roles for miR-34a and miR-16 in cell fate regulation. Sci. Rep. 10, 2511.

Herbst R.S., Morgensztern D. and Boshoff C. (2018). The biology and management of non-small cell lung cancer. Nature 553, 446-454.

Hu S., Cao P., Kong K., Han P., Deng Y., Li F. and Zhao B. (2021). MicroRNA-449a delays lung cancer development through inhibiting KDM3A/HIF-1alpha axis. J. Transl. Med. 19, 224.

Huang L., Liu Z., Hu J., Luo Z., Zhang C., Wang L. and Wang Z. (2020a). MiR-377-3p suppresses colorectal cancer through negative regulation on Wnt/beta-catenin signaling by targeting XIAP and ZEB2. Pharmacol. Res. 156, 104774.

Huang Y., Dai Y., Wen C., He S., Shi J., Zhao D., Wu L. and Zhou H. (2020b). CircSETD3 contributes to acquired resistance to gefitinib in non-small-cell lung cancer by targeting the miR-520h/ABCG2 pathway. Mol. Ther. Nucleic Acids 21, 885-899.

Jiang M., Xu S., Yue W., Zhao X., Zhang L., Zhang C. and Wang Y. (2012). The role of ZFX in non-small cell lung cancer development. Oncol. Res. 20, 171-178.

Lai K.P., Chen J., He M., Ching A.K., Lau C., Lai P.B., To K.F. and Wong N. (2014). Overexpression of ZFX confers self-renewal and chemoresistance properties in hepatocellular carcinoma. Int. J. Cancer 135, 1790-1799.

Leonetti A., Assaraf Y.G., Veltsista P.D., El Hassouni B., Tiseo M. and Giovannetti E. (2019). MicroRNAs as a drug resistance mechanism to targeted therapies in EGFR-mutated NSCLC: Current implications and future directions. Drug Resist. Updat. 42, 1-11.

Li K., Zhu Z.C., Liu Y.J., Liu J.W., Wang H.T., Xiong Z.Q., Shen X., Hu Z.L. and Zheng J. (2013). ZFX knockdown inhibits growth and migration of non-small cell lung carcinoma cell line H1299. Int. J. Clin. Exp. Pathol. 6, 2460-2467.

Li L., Zhang Q. and Lian K. (2020). Circular RNA circ_0000284 plays an oncogenic role in the progression of non-small cell lung cancer through the miR-377-3p-mediated PD-L1 promotion. Cancer Cell Int. 20, 247.

Rhie S.K., Yao L., Luo Z., Witt H., Schreiner S., Guo Y., Perez A.A. and Farnham P.J. (2018). ZFX acts as a transcriptional activator in multiple types of human tumors by binding downstream of transcription start sites at the majority of CpG island promoters. Genome Res. 28, 310-320,

Shah R. and Lester J.F. (2020). Tyrosine kinase inhibitors for the treatment of EGFR mutation-positive non-small-cell lung cancer: A clash of the generations. Clin. Lung Cancer 21, e216-e228.

Shi Y., Au J.S., Thongprasert S., Srinivasan S., Tsai C.M., Khoa M.T., Heeroma K., Itoh Y., Cornelio G. and Yang P.C. (2014). A prospective, molecular epidemiology study of EGFR mutations in Asian patients with advanced non-small-cell lung cancer of adenocarcinoma histology (PIONEER). J. Thorac. Oncol. 9, 154-162.

Song L., Cui Z. and Guo X. (2020). Comprehensive analysis of circular RNA expression profiles in cisplatin-resistant non-small cell lung cancer cell lines. Acta Biochim. Biophys. Sin. (Shanghai) 52, 944-953.

Sun C., Li S., Zhang F., Xi Y., Wang L., Bi Y. and Li D. (2016). Long non-coding RNA NEAT1 promotes non-small cell lung cancer progression through regulation of miR-377-3p-E2F3 pathway. Oncotarget 7, 51784-51814.

Tan J., Wang W., Song B., Song Y. and Meng Z. (2020). Integrative Analysis of three novel competing endogenous RNA biomarkers with a prognostic value in lung adenocarcinoma. Biomed Res. Int. 2020, 2837906.

Travis W.D., Brambilla E., Nicholson A.G., Yatabe Y., Austin J.H.M., Beasley M.B., Chirieac L.R., Dacic S., Duhig E., Flieder D.B., Geisinger K., Hirsch F.R., Ishikawa Y., Kerr K.M., Noguchi M., Pelosi G., Powell C.A., Tsao M.S., Wistuba I. and Panel W.H.O. (2015). The 2015 World Health Organization Classification of lung tumors: Impact of genetic, clinical and radiologic advances since the 2004 classification. J. Thorac. Oncol. 10, 1243-1260.

Wang C.Q., Chen L., Dong C.L., Song Y., Shen Z.P., Shen W.M. and Wu X.D. (2017). MiR-377 suppresses cell proliferation and metastasis in gastric cancer via repressing the expression of VEGFA. Eur. Rev. Med. Pharmacol. Sci. 21, 5101-5111.

Wang J., Li X., Lu L., He L., Hu H. and Xu Z. (2018a). Circular RNA hsa_circ_0000567 can be used as a promising diagnostic biomarker for human colorectal cancer. J. Clin. Lab. Anal. 32, e22379.

Wang Z., Pan L., Yu H. and Wang Y. (2018b). The long non-coding RNA SNHG5 regulates gefitinib resistance in lung adenocarcinoma cells by targetting miR-377/CASP1 axis. Biosci. Rep. 38, BSR20180400.

Wang W., Wang Y., Piao H., Li B., Huang M., Zhu Z., Li D., Wang T., Xu R. and Liu K. (2019a). Circular RNAs as potential biomarkers and therapeutics for cardiovascular disease. PeerJ 7, e6831.

Wang Y., Li Y., He H. and Wang F. (2019b). Circular RNA circ-PRMT5 facilitates non-small cell lung cancer proliferation through upregulating EZH2 via sponging miR-377/382/498. Gene 720, 144099.

Wen C., Xu G., He S., Huang Y., Shi J., Wu L. and Zhou H. (2020). Screening circular RNAs related to acquired gefitinib resistance in non-small cell lung cancer cell lines. J. Cancer 11, 3816-3826.

Westover D., Zugazagoitia J., Cho B.C., Lovly C.M. and Paz-Ares L. (2018). Mechanisms of acquired resistance to first- and second-generation EGFR tyrosine kinase inhibitors. Ann. Oncol. 29, i10-i19.

Wu J., Wei B., Wang Q., Ding Y., Deng Z., Lu X. and Li Y. (2016). ZFX facilitates cell proliferation and imatinib resistance in chronic myeloid leukemia cells. Cell Biochem. Biophys. 74, 277-283.

Xu N., Chen S., Liu Y., Li W., Liu Z., Bian X., Ling C. and Jiang M. (2018). Profiles and bioinformatics analysis of differentially expressed Circrnas in taxol-resistant non-small cell lung cancer cells. Cell. Physiol. Biochem. 48, 2046-2060.

Ye C., Hu Y. and Wang J. (2019). MicroRNA-377 targets zinc finger E-box-binding homeobox 2 to inhibit cell proliferation and invasion of cervical cancer. Oncol. Res. 27, 183-192.

Yu A., Li M., Xing C., Chen D., Wang C., Xiao Q., Zhang L., Pang Y., Wang Y., Zu X. and Liu L. (2020). A comprehensive analysis identified the key differentially expressed circular ribonucleic acids and methylation-related function in pheochromocytomas and paragangliomas. Front. Genet. 11, 15.

Zha W., Cao L., Shen Y. and Huang M. (2013). Roles of MiR-144-ZFX pathway in growth regulation of non-small-cell lung cancer. PLoS One 8, e74175.

Zhang J., Zhao M., Xue Z.Q., Liu Y. and Wang Y.X. (2016). miR-377 inhibited tumorous behaviors of non-small cell lung cancer through directly targeting CDK6. Eur. Rev. Med. Pharmacol. Sci. 20, 4494-4499.

Zhang J., Li Y., Dong M. and Wu D. (2017). Long non-coding RNA NEAT1 regulates E2F3 expression by competitively binding to miR-

377 in non-small cell lung cancer. Oncol. Lett. 14, 4983-4988.

Zhong Y., Lin H., Li Q., Liu C. and Shen J. (2021). CircRNA_100565 contributes to cisplatin resistance of NSCLC cells by regulating proliferation, apoptosis and autophagy via miR-337-3p/ADAM28 axis. Cancer Biomark 30, 261-273.

Zhu X., Han J., Lan H., Lin Q., Wang Y. and Sun X. (2020). A novel circular RNA hsa_circRNA_103809/miR-377-3p/GOT1 pathway regulates cisplatin-resistance in non-small cell lung cancer (NSCLC). BMC Cancer 20, 1190.

Zhu X., Kudo M., Huang X., Sui H., Tian H., Croce C.M. and Cui R. (2021). Frontiers of microRNA signature in non-small cell lung cancer. Front. Cell Dev. Biol. 9, 643942.

Accepted February 8, 2022